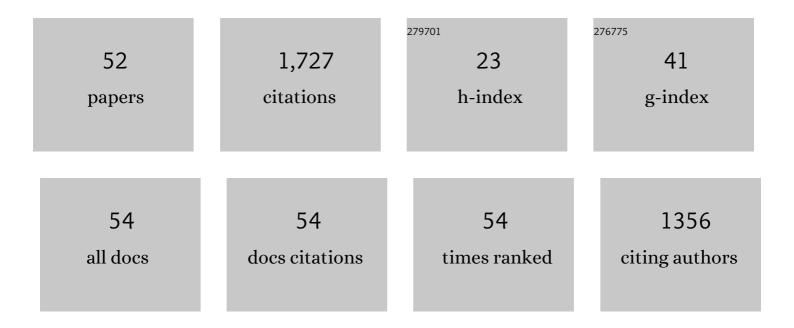
Kewei Gao

List of Publications by Year in descending order

Source: https://exaly.com/author-pdf/2684913/publications.pdf Version: 2024-02-01



KEWEL CAO

#	Article	IF	CITATIONS
1	Study of Thermal Stress Fluctuations at the Die-Attach Solder Interface Using the Finite Element Method. Electronics (Switzerland), 2022, 11, 62.	1.8	6
2	High-throughput technique for stress corrosion cracking susceptibility measurements based on film-induced stress. Vacuum, 2022, 203, 111275.	1.6	2
3	Synthesis and Enhanced Electro-Magnetic Wave Absorbing Properties of Reduced Graphene Oxide-Fe3O4-Polyaniline Ternary Nano-Composites. Science of Advanced Materials, 2021, 13, 473-480.	0.1	1
4	Enhanced Electro-Magnetic Wave Absorbing Properties of Fe3O4-Polyaniline Nano-Composites. Science of Advanced Materials, 2021, 13, 938-943.	0.1	2
5	Effect of 2D nanocrystalline ZnAl-LDHs films with different orientations on anticorrosion performance of magnesium alloys. Materials Letters, 2021, 293, 129708.	1.3	6
6	Analysis of Environmental Factors Affecting the Atmospheric Corrosion Rate of Low-Alloy Steel Using Random Forest-Based Models. Materials, 2020, 13, 3266.	1.3	12
7	Corrosion rate prediction and influencing factors evaluation of low-alloy steels in marine atmosphere using machine learning approach. Science and Technology of Advanced Materials, 2020, 21, 359-370.	2.8	55
8	One-Step in Situ Synthesis of Reduced Graphene Oxide/Zn–Al Layered Double Hydroxide Film for Enhanced Corrosion Protection of Magnesium Alloys. Langmuir, 2019, 35, 6312-6320.	1.6	63
9	Understanding the general and localized corrosion mechanisms of Cr-containing steels in supercritical CO2-saturated aqueous environments. Journal of Alloys and Compounds, 2019, 792, 328-340.	2.8	25
10	Tribo-corrosion and Albumin Attachment of Nitrogen Ion-Implanted CoCrMo Alloy During Friction Onset. Journal of Materials Engineering and Performance, 2019, 28, 363-371.	1.2	5
11	Residual stress control in CrAlN coatings deposited on Ti alloys. Ceramics International, 2018, 44, 4653-4659.	2.3	18
12	Corrosion of low alloy steel containing 0.5% chromium in supercritical CO2-saturated brine and water-saturated supercritical CO2 environments. Applied Surface Science, 2018, 440, 524-534.	3.1	40
13	Effect of flow rate on localized corrosion of X70 steel in supercritical CO2 environments. Corrosion Science, 2018, 136, 339-351.	3.0	55
14	Design and fabrication of enhanced corrosion resistance Zn-Al layered double hydroxides films based anion-exchange mechanism on magnesium alloys. Applied Surface Science, 2017, 404, 246-253.	3.1	95
15	Effect of exposure angle on the corrosion behavior of X70 steel under supercritical CO 2 and gaseous CO 2 environments. Corrosion Science, 2017, 121, 57-71.	3.0	28
16	Effects of anions on corrosion behaviour of carbon steel in simulated groundwater in China. Corrosion Engineering Science and Technology, 2017, 52, 84-89.	0.7	3
17	The Regular Interaction Pattern among Odorants of the Same Type and Its Application in Odor Intensity Assessment. Sensors, 2017, 17, 1624.	2.1	40
18	Applications and Thermodynamic Analysis of Equilibrium Solution for Secondary Phases in Ti–N–C Gear Steel System with Nano-Particles. Metals, 2017, 7, 110.	1.0	5

Kewei Gao

#	Article	IF	CITATIONS
19	Pronounced effect of ZnTe nanoinclusions on thermoelectric properties of Cu2â^'x Se chalcogenides. Science China Materials, 2016, 59, 135-143.	3.5	17
20	Annealing temperature effects on optical and photoelectric properties of sputtered indium-doped PbSe thin films. Journal of Materials Science: Materials in Electronics, 2016, 27, 1670-1678.	1.1	6
21	Corrosion of low alloy steel and stainless steel in supercritical CO 2 /H 2 O/H 2 S systems. Corrosion Science, 2016, 111, 637-648.	3.0	78
22	Interface and Strain Energy Revolution Texture Map To Predict Structure and Optical Properties of Sputtered PbSe Thin Films. ACS Applied Materials & Interfaces, 2016, 8, 625-633.	4.0	29
23	Effect of small amount of H 2 S on the corrosion behavior of carbon steel in the dynamic supercritical CO 2 environments. Corrosion Science, 2016, 103, 132-144.	3.0	108
24	Effects of alloyed Cr and Cu on the corrosion behavior of low-alloy steel in a simulated groundwater solution. Corrosion Science, 2016, 102, 114-124.	3.0	54
25	Cd-doping a facile approach for better thermoelectric transport properties of BiCuSeO oxyselenides. RSC Advances, 2016, 6, 33789-33797.	1.7	48
26	Residual Stress and Surface Energy of Sputtered TiN Films. Journal of Materials Engineering and Performance, 2015, 24, 1185-1191.	1.2	39
27	Insitu grown superhydrophobic Zn–Al layered double hydroxides films on magnesium alloy to improve corrosion properties. Applied Surface Science, 2015, 337, 172-177.	3.1	125
28	Corrosion behaviors of steels under supercritical CO2 conditions. Corrosion Reviews, 2015, 33, 151-174.	1.0	24
29	Thickness effects on optical and photoelectric properties of PbSeTeO quaternary thin films prepared by magnetron sputtering. Journal of Materials Science: Materials in Electronics, 2015, 26, 7873-7881.	1.1	8
30	Formation mechanism and protective property of corrosion product scale on X70 steel under supercritical CO 2 environment. Corrosion Science, 2015, 100, 404-420.	3.0	101
31	Adhesion of Sputtered Nickel Films on Polycarbonate Substrates. Journal of Materials Engineering and Performance, 2014, 23, 786-790.	1.2	10
32	TiN-Coating Effects on Stainless Steel Tribological Behavior Under Dry and Lubricated Conditions. Journal of Materials Engineering and Performance, 2014, 23, 1263-1269.	1.2	13
33	The effect of ion implantation on tribology and hot rolling contact fatigue of Cr4Mo4Ni4V bearing steel. Applied Surface Science, 2014, 305, 93-100.	3.1	31
34	Fracture Toughness and Adhesion of Transparent Al:ZnO Films Deposited on Glass Substrates. Journal of Materials Engineering and Performance, 2013, 22, 3161-3167.	1.2	7
35	Discussion of the CO2 corrosion mechanism between low partial pressure and supercritical condition. Corrosion Science, 2012, 59, 186-197.	3.0	160
36	A novel observation of the interaction between the macroelastic stress and electrochemical corrosion of low carbon steel in 3.5wt% NaCl solution. Electrochimica Acta, 2012, 85, 283-294.	2.6	44

Kewei Gao

#	Article	lF	CITATIONS
37	Failure analysis of the oil transport spiral welded pipe. Engineering Failure Analysis, 2012, 25, 169-174.	1.8	15
38	The relationship between fracture toughness of CO2 corrosion scale and corrosion rate of X65 pipeline steel under supercritical CO2 condition. International Journal of Greenhouse Gas Control, 2011, 5, 1643-1650.	2.3	41
39	AlTiN layer effect on mechanical properties of Ti-doped diamond-like carbon composite coatings. Thin Solid Films, 2011, 519, 5353-5357.	0.8	14
40	Annealing effects on microstructure and mechanical properties of sputtered multilayer Cr(1â^'x)AlxN films. Thin Solid Films, 2011, 519, 5831-5837.	0.8	14
41	Microstructure and mechanical properties of Ti/AlTiN/Ti-diamondlike carbon composite coatings on steel. Journal of Materials Research, 2010, 25, 2159-2165.	1.2	3
42	Investigation of microstructure and mechanical properties of multi-layer Cr/Cr2O3 coatings. Thin Solid Films, 2009, 517, 1922-1927.	0.8	44
43	Mechanical properties of CO2 corrosion product scales and their relationship to corrosion rates. Corrosion Science, 2008, 50, 2796-2803.	3.0	115
44	Corrosion behaviors of the exposed side and underside of low alloy weathering steel in Qingdao and Wanning for 18 months. Acta Metallurgica Sinica (English Letters), 2008, 21, 425-436.	1.5	5
45	Microstructure and mechanical properties of chromium oxide coatings. Journal of Materials Research, 2007, 22, 3531-3537.	1.2	54
46	Stress corrosion cracking and its anisotropy of a PZT ferroelectric ceramics. Science Bulletin, 2003, 48, 1203-1206.	1.7	0
47	Interface Stability in Diffusion Couple of L1 ₀ type TiAl and L1 ₂ type (Al,) Tj ETQq1 1	0.784314 0.4	rgBT /Over
48	Investigation of stress corresion cracking under anodic dissolution control. Science Bulletin, 2001, 46, 717-722.	1.7	10
49	Stress corrosion cracking relation with dezincification layer-induced stress. Metallurgical and Materials Transactions A: Physical Metallurgy and Materials Science, 2001, 32, 1309-1312.	1.1	32
50	Fracture mechanism of TiAl intermetallics caused by hydride and atomic hydrogen. Science in China Series D: Earth Sciences, 1999, 42, 511-520.	0.9	3
51	Corrosion-enhanced dislocation emission and motion resulting in initiation of stress corrosion cracking. Science in China Series D: Earth Sciences, 1997, 40, 235-242.	0.9	10
52	Achieving Low Yield Ratio in High‣trength Steel by Tuning Multiple Microstructures. Steel Research International, 0, , 2100415.	1.0	1